Development and statistical validation of an image processing system for total ammonia nitrogen monitoring in aquaculture

Kritsada Puangsuwan*, Jaruphat Wongpanich, Rattanasak Hama

(*Faculty of Science and Industrial Technology, Prince of Songkla University, Surat Thani Campus, Surat Thani 84000, Thailand*)

Abstract: Aquaculture has become essential for global food security and economic growth, but its productivity relies heavily on effective water quality management. Total ammonia nitrogen (TAN) concentration is a key parameter, as high concentrations can harm aquatic life and disrupt cultivation systems. Conventional TAN measurement methods including colorimetric tests, spectrophotometry, electrochemical techniques, and biological assays offer high analytical accuracy but remain costly, complex, and often inaccessible for small-scale farmers. To overcome these limitations, this study developed a low-cost, TAN monitoring prototype using image processing techniques integrated with a Raspberry Pi microcontroller. Standard TAN solutions (0-5 mg/L) were prepared to construct regression models based on red (R) green (G) blue (B) color values extracted from captured images. Validation experiments showed that although both the R and G channel models provided strong predictive capability, the G channel model demonstrated superior practical performance. The G channel achieved the coefficient of determination (R^2)=0.969, mean absolute error (MAE)=0.535 mg/L, root mean squared error (RMSE)=0.805 mg/L, a sensitivity of 1.397, and a limit of detection (LOD) of 0.215 mg/L, delivering stable and consistent predictions in the concentration range of 0.2-2.0 mg/L. In contrast, the R channel model, despite achieving higher numerical accuracy, exhibited greater drift at higher TAN concentrations, reducing its reliability in operational settings. The prototype system displays TAN values on a liquid crystal display (LCD) screen and sends notifications via the LINE application, enabling aquaculturists to respond promptly to potential water quality risks. By offering an affordable, accessible, and user-friendly alternative to conventional analytical methods, the proposed system supports more effective water quality management and contributes to the sustainable development of aquaculture practices.

Keywords: total ammonia nitrogen, image processing, aquaculture water quality, mathematic model

DOI: 10.25165/j.ijabe.20261901.10224

Citation: Puangsuwan K, Wongpanich J, Hama R. Development and statistical validation of an image processing system for total ammonia nitrogen monitoring in aquaculture. Int J Agric & Biol Eng, 2026; 19(1): 26–32.

1 Introduction

Aquaculture has become increasingly important as natural aquatic resources decline due to overfishing, environmental degradation, and rising demand for aquatic products. In Thailand, aquaculture contributes significantly to the economy, with exports exceeding two hundred billion Baht annually[1]. The productivity of aquaculture systems depends heavily on water quality management, with critical factors including temperature, salinity, turbidity, pH, and nitrogen compounds, which directly influence the growth, reproduction, and survival of aquatic organisms[2-4]. Nitrogen, an essential nutrient, exists in aquatic systems mainly as un-ionized ammonia (NH_3), which is highly toxic, and ionized ammonium (NH_4^+), which is less toxic. The balance between these forms is governed by pH, temperature, and salinity, with NH_4^+ dominating below pH 8.75 and NH_3 above pH 9.75. Total ammonia nitrogen (TAN), the sum of both species, is routinely monitored because NH_3 can cause toxicity at concentrations as low as 0.06 mg/L and cause gill and kidney damage to fish. If the concentration is higher than 0.6 mg/L, it could be fatal to some types of fish[5,6], with toxicity increasing at higher pH due to chemical equilibrium shifts toward greater NH_3 presence, described by the reaction $NH_3+H_2O \rightleftharpoons NH_4^+ + OH^-$[4-9]. TAN in aquaculture ponds originates from feed residues, animal excretion, decaying organisms, and plant debris, and its accumulation over time can be toxic to aquatic animals[2-4]. In conventional aquaculture, water exchange or reduced feeding is often implemented to control the TAN concentration in water and prevent it from becoming excessively high. Therefore, effective management of water quality in breeding ponds is of utmost importance[10-12].

Currently, a widely adopted method for analyzing TAN concentration in water is the colorimetric method. This involves adding a chemical reagent to the water, which reacts with TAN to produce a colored compound. The intensity of the color is then compared to a standard color chart, such as blue tones, brown, or yellow-green, to determine the TAN concentration[13-16]. Another method, particularly when precise measurement of ammonia quantity is required, involves using either an ammonia test kit or a spectrophotometer, which measures light absorbance[14-19]. Both methods are accurate, but the latter can be expensive and may exceed the affordability of small-scale aquaculturists[14]. In addition to these optical techniques, several electrochemical and biological methods have been developed for ammonia and TAN determination in both natural and engineered aquatic environments. Electrochemical approaches can provide *in situ* measurements with rapid response times and relatively low detection limits. These approaches include ion-selective electrodes, potentiometric and

Received date: 2025-09-28 **Accepted date:** 2026-01-04

Biographies: Jaruphat Wongpanich, PhD, research interest: nanoparticles and chemistry synthesis, Email: jaruphat.w@psu.ac.th; **Rattanasak Hama**, Assistant Professor, research interest: applied mathematics, Email: rattanasak.h@psu.ac.th.

***Corresponding author: Kritsada Puangsuwan**, Assistant Professor, research interest: electronics technology for agriculture and artificial intelligence of things. Faculty of Science and Industrial Technology, Prince of Songkla University, Surat Thani Campus, Surat Thani 84000, Thailand, Tel: +660-840524595, Email: kritsada.pu@psu.ac.th.

amperometric sensors, and voltammetric probes. Nevertheless, their long-term use in aquaculture environments is hindered by electrode fouling, calibration drift, ion cross-interference, and the need for frequent recalibration and controlled operating conditions. These drawbacks reduce their reliability for continuous field deployment[20,21]. Moreover, biological and enzymatic methods, such as microbial nitrification-based biosensors and enzyme-coupled assays, also offer excellent molecular selectivity and can reflect biologically relevant toxicity. However, they typically require strict environmental control (temperature, pH, nutrient conditions) which exhibit limited operational stability, and degrade rapidly when exposed to real conditions. These can limit their suitability for routine monitoring in small- and medium-scale farms[22,23]. Advanced materials-based approaches such as polydiacetylene (PDA) sensors and plasmonic nanostructures have further improved sensitivity. However, PDA sensors often require controlled laboratory conditions to maintain chromatic stability and have not been fully integrated into compact, field-ready devices[24]. Beyond these aforementioned techniques, image-based and digital colorimetric methods have gained increasing attention due to their low hardware cost, minimal operational complexity, and compatibility with embedded processing systems. Take smartphone-based colorimetry for instance, which has demonstrated that RGB or HSV (hue, saturation, and value) features derived from reagent-induced color changes can be used to estimate TAN concentrations with reasonable accuracy in portable devices[25-27]. However, this technique remains vulnerable to turbidity, ambient illumination variability, and inconsistent manual handling, which adversely affect reliability in real aquaculture environments[2,3]. Similarly, image processing methods using DSLR or PC cameras have achieved high accuracy, yet their reliance on high-quality imaging equipment and controlled lighting restricts their practicality for small-scale aquaculturists[28]. IoT-enabled monitoring systems integrating Raspberry Pi and OpenCV libraries provide automated detection, but their complexity and cost limit widespread implementation among smallholder farms[29]. Taken together, these limitations reveal a clear need for a low-cost, portable, and robust TAN monitoring system that can operate reliably under real aquaculture conditions without dependence on expensive instrumentation, complex reagent handling, or specialized technical expertise.

To address these challenges, this research proposes a system for monitoring TAN concentrations in aquaculture using image processing techniques. The system employs RGB color analysis of water samples, with color channel regression models validating accurate TAN estimation. Designed to be efficient and affordable for small-scale aquaculturists, the prototype captures images of water samples, processes them via a microcontroller, displays results on an LCD screen, and transmits data through the LINE application for convenient monitoring.

2 Methodology

2.1 Prototype system workflow for monitoring TAN concentration in aquaculture water

Figure 1 presents the workflow diagram of the proposed prototype system for monitoring TAN concentration in water. The system integrates Python OpenCV with a Raspberry Pi 4 microcontroller, which operates as a compact platform capable of image processing. The workflow begins with sample preparation, where standard TAN solutions were prepared at concentrations of 0, 0.2, 0.4, 0.6, 1, 2, 3, and 5 mg/L. These reference concentrations were obtained using a commercial Ammonium test kit, which induced distinct color changes in the water samples. Two sets of standard TAN solutions were employed. The first set was used for model training, where the RGB color values extracted from the images were processed through a mathematical regression model. This model was embedded into the microcontroller to enable on-device computation of TAN concentration. The second set of standard TAN solutions was used for validation, ensuring that the derived model could reliably estimate TAN concentrations under different conditions.

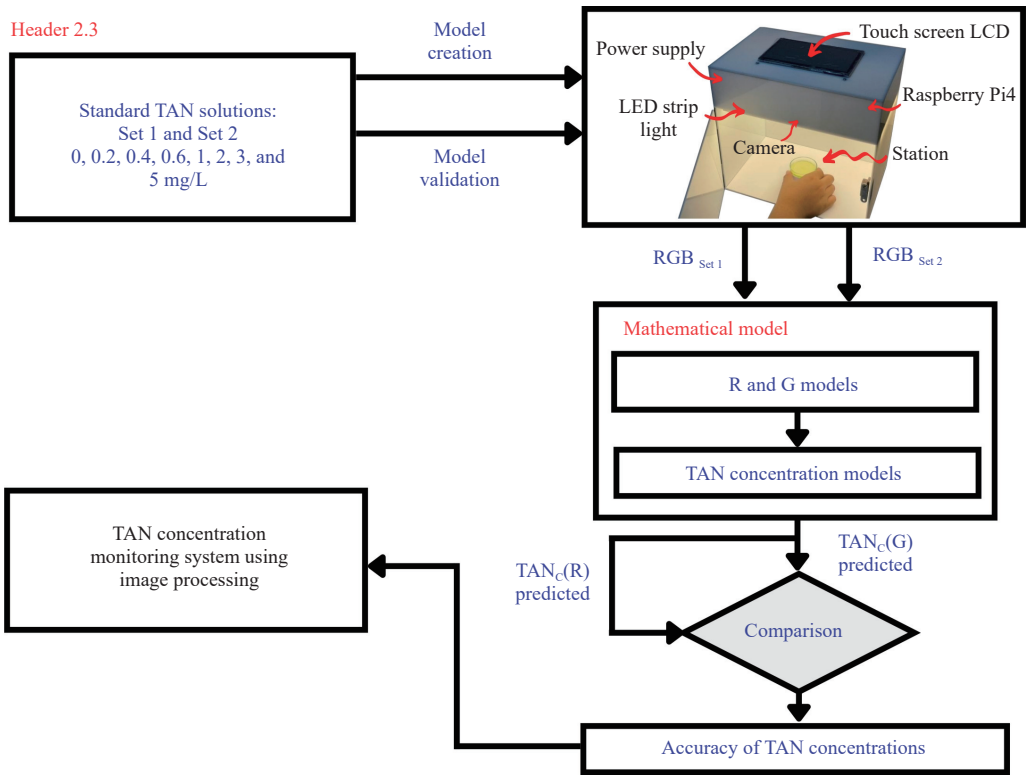

Figure 1 Overview of the system workflow

2.2 Prototype system for monitoring TAN concentration in aquaculture water using image processing

The prototype system for measuring TAN concentration in aquaculture water using image processing was designed as a closed rectangular chamber with dimensions of 20×31×28 cm³. The chamber was fabricated from 5 mm-thick white opaque acrylic sheets, providing structural rigidity and light diffusion to eliminate external illumination interference. This configuration ensures that the Raspberry Pi Camera V2 (8 MP, fixed-focus lens) captures water sample images under consistent lighting conditions and accurately distinguishes RGB color intensities from the controlled background, thereby reducing color detection errors. The hinged upper section of the chamber allows convenient access for integrating electronic components, including the Raspberry Pi 4 microcontroller (4 GB RAM), a 5-inch LCD display, and a 5 V/3 A regulated power supply. Uniform illumination is maintained by a built-in LED array with a fixed color temperature of 6500 K, while the front panel incorporates a precision-fitted door to insert the water sample cuvette at the designated focal plane station, ensuring repeatable alignment with the camera optics. The matte acrylic interior minimizes specular reflections and enhances image stability. The complete prototype setup is shown in Figure 2.

The prototype system operates through four integrated modules, as illustrated in Figure 3. First, water samples subjected to ammonium test kit reactions were captured by the Raspberry Pi Camera V2, producing observable color changes. The images were then processed by a Raspberry Pi 4 microcontroller using Python OpenCV, where RGB values were extracted and analyzed through mathematical regression models to estimate TAN concentration. A regulated switching power supply (12 V_{DC}, 5 A, 60 W) drives the LED strip lights installed inside the chamber, ensuring stable and uniform illumination for accurate image acquisition. The processed results were displayed locally on an LCD touch screen and simultaneously transmitted via Wi-Fi to an API server, with notifications delivered to users through the Line Notify application for effective aquaculture monitoring and decision-making.

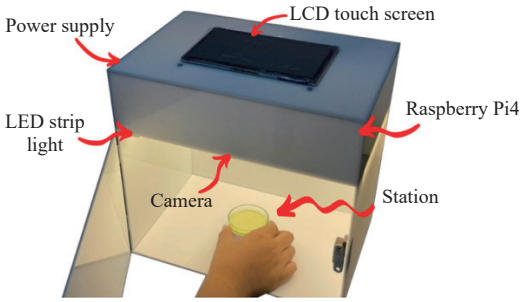

Figure 2 Prototype system for TAN concentration monitoring of aquaculture water

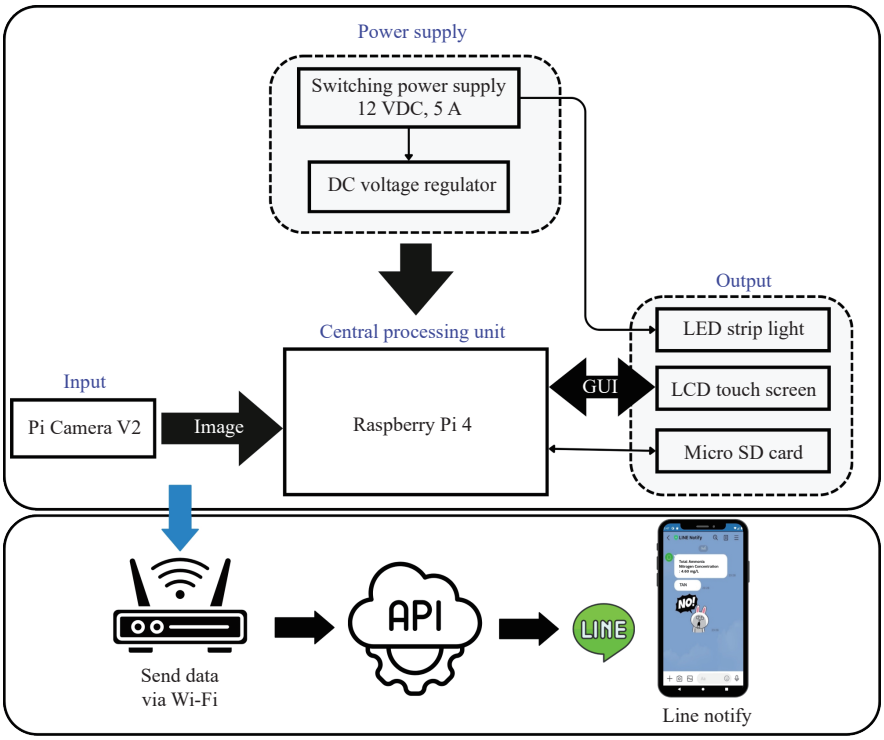

Figure 3 Block diagram of the prototype system for monitoring TAN concentration of aquaculture water

2.3 Preparation of standard TAN solutions for prototype development

The analysis of TAN concentration in water using image processing techniques requires a chemical process to establish the relationship between concentration values and the color of the tested water samples for developing a mathematical model. In this study, two sets of standard TAN solutions were prepared where the first set was used for developing the mathematical model, and the second set was employed for validating its accuracy. The standard TAN solutions were prepared as follows: Firstly, a stock solution of 1000 mg/L of TAN was prepared by dissolving 3.92 g of NH_4Cl in 1000 mL of deionized water. Then, standard TAN solutions were then prepared by dilution of the stock solution to give a concentration of 0, 0.2, 0.4, 0.6, 1, 2, 3, and 5 mg/L. The TAN concentrations were measured using the v-color 9750 Ammonium test kit from V-unique, U.S.A. (Figure 4a) by rinsing the test tubes with sample water, then filled with 5 mL of the sample water. Ten drops of solution A-1 were added to the test tube and stirred to make a homogenous solution. Then, two drops of solution A-2 were added to the test tube, stirred, and left to complete the reaction for 5 min at room temperature. Furthermore, five drops of solution A-3 were added to the test tube, stirred, and left to complete the reaction

for 7 min at room temperature. When the chemical reactions are complete for all concentrations, the water will exhibit different colors corresponding to the varying concentrations of ammonia in the water (Figure 4b). To ensure high reproducibility and minimize the influence of environmental variables, this system utilizes pre-buffered reagents designed to maintain the reaction mixture at an optimal pH, thereby mitigating potential fluctuations caused by sample acidity or alkalinity. Furthermore, the reaction kinetics were standardized by strictly adhering to the manufacturer's recommended reaction time of 5-7 min before optical measurement. By employing this standardized chemical protocol, the influence of pH variation and reaction time was effectively controlled, allowing the study to focus on the performance of the system.

a. Preparation of standard TAN solutions at concentrations of 0-5 mg/L

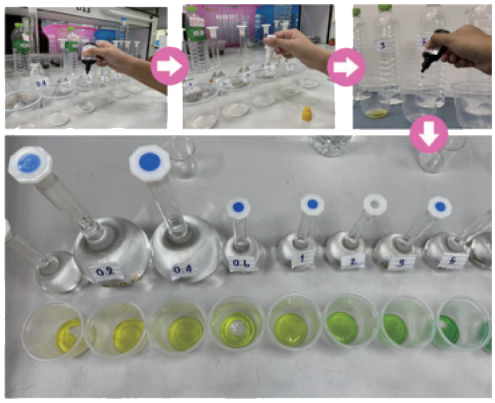

b. TAN test kit induced color change

Figure 4 Standard TAN solution preparation for prototype development

2.4 Mathematic model equation for the TAN concentration measurement using the system

This section describes the methodology used to develop the regression model for estimating TAN concentration, along with a systematic specification of its parameters. Furthermore, an independent validation test was conducted using a new set of samples with varying TAN concentrations to rigorously assess the model's predictive performance and accuracy. In this study, the standard TAN solutions were prepared at concentrations of 0, 0.2, 0.4, 0.6, 1, 2, 3, and 5 mg/L. Each TAN concentration level was tested using the ammonium test kit until a visible color change occurred, as illustrated in Figure 5.

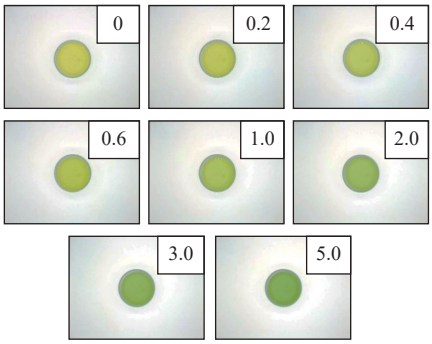

Figure 5 Optical images of standard TAN solutions tested using an ammonium test kit for model development

The system cropped the central region of each sample image, with the cropping area precisely aligned at the image center. To ensure measurement reliability and minimize potential variability, each concentration level was tested in ten repetitions. The RGB values extracted from these images were plotted against the corresponding TAN concentrations to assess their individual relationships, as shown in Figure 6. In this figure, each RGB component was independently plotted against the transformed variable 1/(TAN+1). Correlation analysis revealed strong associations for the Green (G) and Red (R) channels, with correlation coefficients of 0.927 and −0.892, respectively. By contrast, the Blue (B) channel showed only a negligible correlation (0.087), indicating minimal variation and no apparent trend, and was therefore excluded from further modeling.

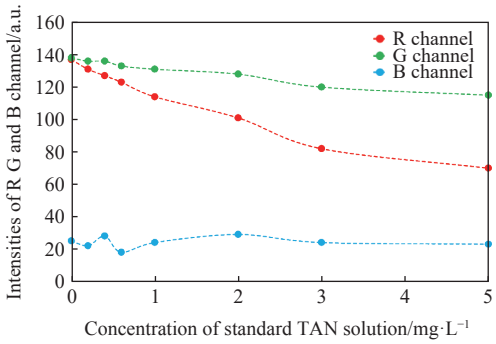

Figure 6 Plot of RGB channel intensities against standard TAN concentrations

Based on these observations, the G and R channels were selected for mathematical modeling. Their intensity values, extracted from the standard TAN solution images in Figure 6, were used to construct regression plots against $1/(TAN_C+1)$, where TAN_C represents the value of TAN concentration. Subsequently, linear regression was applied to both channels, as represented in Equations (1) and (2):

$$G = \frac{26.013}{TAN_C+1}+115.24 \quad (1)$$

$$R = \frac{78.670}{TAN_C+1}+67.134 \quad (2)$$

The G and R variables, representing the G and R channel intensities, were empirically obtained through experimental calibration and nonlinear regression. Both equations describe inverse relationships, with channel intensities asymptotically approaching baseline values as TAN_C increases. From the models expressed in Equations (3) and (4), the corresponding plots in Figure 7 illustrate the intensity of the G and R components as functions of TAN_C in the samples. By rearranging both equations, the TAN_C can further be expressed as a function of the G and R channel intensities, as shown in the derived equations:

$$TAN_C=\frac{26.013}{G-115.24}-1 \quad (3)$$

$$TAN_C=\frac{78.670}{R-67.134}-1 \quad (4)$$

2.5 Statistical evaluation metrics

To evaluate the predictive performance of the proposed models, three statistical indicators were employed: mean absolute error (MAE), root mean squared error (RMSE), and the coefficient of determination (R^2). These metrics are widely adopted in regression analysis to quantify the accuracy, precision, and goodness-of-fit of predictive models[30]. These indicators were calculated as follows:

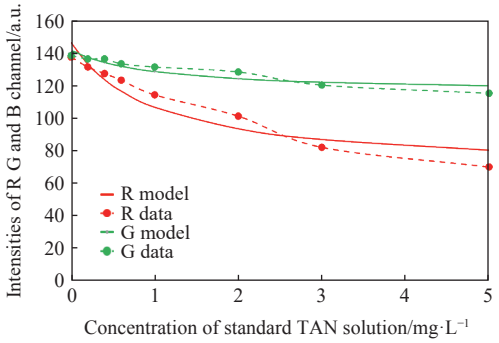

Figure 7 Plot of experimental and modeled R and G channel intensities versus standard TAN concentrations

$$\mathrm{MAE}=\frac{1}{n}\sum_{i=1}^{n}|y_i-\hat{y}_i| \tag{5}$$

$$\mathrm{RMSE}=\sqrt{\frac{1}{n}\sum_{i=1}^{n}(y_i-\hat{y}_i)^2} \tag{6}$$

$$R^2=1-\frac{\frac{1}{n}\sum_{i=1}^{n}(y_i-\hat{y}_i)^2}{\frac{1}{n}\sum_{i=1}^{n}\left(y_i-\bar{y}_i\right)^2} \tag{7}$$

where, y_i is the reference TAN concentration, mg/L; $\hat{y}_i$ the numerical TAN concentration predicted by the model for the i-th sample, mg/L; $\bar{y}_i$ the mean reference value, mg/L; and n the number of samples. After establishing baseline accuracy, the sensing characteristics of each model were quantified beginning with sensitivity, defined as the regression slope (a) in Equation (8):

$$\text{Sensitivity}=a \tag{8}$$

which represents the change in predicted TAN per unit increase in true concentration. The limit of detection (LOD) was then calculated from the standard deviation of the blank signal (σ_{blank}) and the model sensitivity using Equation (9):

$$\mathrm{LOD}=\frac{3\sigma_{\text{blank}}}{\mathrm{a}} \tag{9}$$

indicating the minimum concentration distinguishable above noise.

Precision was evaluated through the distribution of residuals ($y_i-\hat{y}_i$). The detection range, defined in Equation (10):

$$\text{Detection range}=(C_{\text{LOD}},C_{\text{drift}}) \tag{10}$$

was established as the interval between the LOD boundary C_{LOD} and the upper concentration limit C_{drift} at which systematic drift or nonlinear deviation emerged. Finally, stability, described by Equation (11):

$$\text{Stability}=f(\Delta\text{residuals, drift, variance}) \tag{11}$$

was assessed by analyzing drift patterns and residual variance across repeated trials, with models exhibiting lower drift and smaller fluctuations considered more operationally robust. MAE and RMSE, R^2, sensitivity, LOD, precision, detection range, and stability provide a rigorous, multi-parameter framework for evaluating the analytical performance of the image-based TAN sensing models.

3 Results and discussion

3.1 Evaluation of TAN model performance against measured TAN concentrations

In this section, a validation experiment was conducted to evaluate the reliability of the proposed models using a second set of standard TAN solutions prepared at eight concentration levels: 0, 0.2, 0.4, 0.6, 1, 2, 3, and 5 mg/L, as described in Section 2.3. Each concentration was tested in 10 replicates by capturing images with a Raspberry Pi Camera V2, followed by processing the R and G channel values using a Raspberry Pi 4 microcontroller. These data were employed to test the R and G models based on Equations (1) and (2), respectively, as illustrated in Figure 8. The resulting outputs were subsequently employed to compute the correlation between the $\mathrm{TAN_C}$ predicted by the models, based on Equations (3) and (4), and the standard reference values, as illustrated in Figure 9. Finally, the accuracy and error of both models were analyzed to identify the most effective model for correlating TAN concentration with colorimetric data, which was then integrated into the intelligent embedded system of the prototype device.

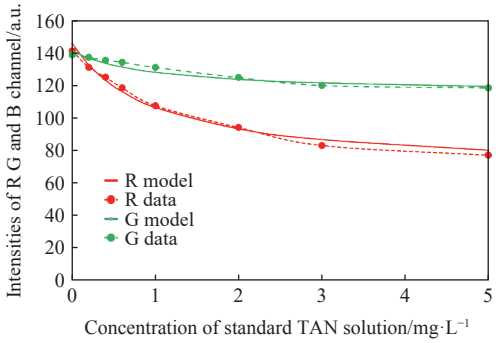

Figure 8 Plot comparing modeled R and G channel intensities against two independent sets of validation samples

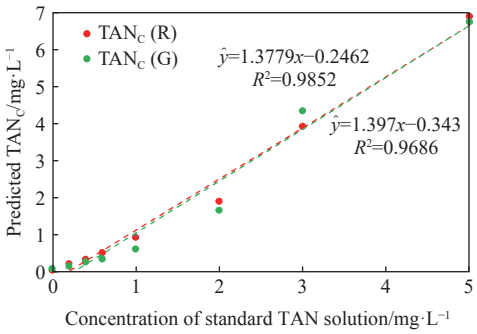

Figure 9 Regression analysis of R and G channel models against standard TAN concentrations

In Figure 9, the regression analysis compares the predicted TAN concentrations derived from the R and G channel responses against the reference standard solutions. The R channel yielded the regression equation $\hat{y}=1.3779x-0.2462$ with $R^2=0.985$, indicating excellent linearity. Likewise, G channel produced $\hat{y}=1.397x-0.343$ with $R^2=0.969$, demonstrating similarly strong agreement with the reference values. The regression slopes, representing the sensitivity of the system, were 1.3779 for the R channel and 1.397 for the G channel, reflecting a strong increase in predicted signal per unit increase in TAN concentration. Slopes greater than unity further suggest a proportional overestimation trend at higher concentrations, which is consistent with the systematic drift observed in both datasets. The analytical performance of each

model, evaluated through precision metrics, showed that the R channel achieved an MAE of 0.398 mg/L and RMSE of 0.747 mg/L, while the G channel obtained an MAE of 0.535 mg/L and RMSE of 0.805 mg/L. The calculated limits of detection (LOD) were 0.155 mg/L for the R channel and 0.215 mg/L for the G channel, indicating that both channels are capable of detecting low TAN concentrations. However, the most reliable and stable predictions for both channels occur within the practical detection range of 0.2–2 mg/L, where prediction errors remain minimal and data points adhere closely to the identity line. In terms of stability, the G channel model demonstrated a more uniform alignment with the identity line across the entire concentration range, particularly in the upper region where the R channel model exhibited more pronounced overestimation. This increased stability in the G channel response is likely attributable to more consistent spectral sensitivity, reduced reagent coloration saturation, and lower noise propagation during image acquisition. Overall, the findings presented in Figure 9 indicate that both models possess strong predictive capability; however, the G channel model provides a more favorable balance between sensitivity, precision, LOD performance, and operational stability. These characteristics make the G channel model more suitable for integration into the embedded prototype system to support reliable TAN monitoring under practical aquaculture operating conditions.

The primary limitation of the proposed method is its relatively narrow linear range (0.2-2.0 mg/L) and an LOD of 0.215 mg/L. In the context of aquaculture, TAN requires rigorous monitoring where the concentrations of un-ionized NH_3 as low as 0.06 mg/L can induce chronic toxicity and lead to gill and kidney damage in fish[5,6]. It is noted that the current LOD of 0.215 mg/L exceeds this lower threshold for chronic sub-lethal effects. However, the method is highly effective for detecting acute toxicity levels, as TAN concentrations exceeding 0.6 mg/L are often fatal to various fish species[5,6]. Consequently, while this system may not be suitable for trace-level monitoring of early-stage chronic exposure, it serves as a robust screening tool for identifying immediate and lethal threats in aquatic environments. Future development will focus on enhancing sensitivity to encompass the sub-lethal range (<0.1 mg/L) to broaden the system's applicability.

3.2 The TAN prototype system

The home screen displayed on the LCD touch screen provides a graphical user interface that receives image data from the Raspberry Pi Camera V2, as shown in Figure 10a. The system outputs the analysis results in two forms. Firstly, the TAN concentration, expressed in mg/L, was calculated using the embedded regression model. Secondly, the system presents an image of the water being tested for TAN concentration. Additionally, the Raspberry Pi 4 transmits the concentration values via Wi-Fi to an API server, enabling notifications through the LINE application, as illustrated in Figure 10b. This integration supports both local visualization and remote monitoring, enhancing the reliability of TAN concentration management in aquaculture water.

3.3 Comparative performance analysis

To evaluate the proposed system with the current technological studies, a comparative analysis was conducted against recent colorimetric methods for TAN detection, as shown in Table 1. While some trace-level sensors offer lower detection ranges of 0-0.45 mg/L, the study lacks the dynamic range required for active aquaculture systems where levels frequently exceed 1.0 mg/L[13]. Conversely, the method of this study provides a reliable range of 0.2-2.0 mg/L that effectively measures the critical toxicity thresholds. Furthermore, this study's validation using standard solutions yielded an R^2 of 0.969, comparable to similar image-based systems[7], confirming its utility as a low-cost screening tool.

a. b.

Figure 10 The home LCD touch screen display (a) and LINE notification for aquaculturists (b)

Table 1 Comparative analysis of sensor performance

Study	Sample matrix	Linear range/ mg·L^{-1}	LOD/ mg·L^{-1}	Accuracy/Precision
Proposed system	Standard TAN solutions	0.20-2.00	0.215	R^2=0.969, RMSE=0.805 mg/L (G-channel)
Garcia et al.[7]	Prepared samples	0.00-3.00	Not stated	Avg. error=0.137 mg/L
Jiang & Tao[13]	Natural water	0.00-0.45	Not stated	R^2=0.999 (High linearity)

4 Conclusions

This study developed and validated a prototype system for monitoring TAN in aquaculture water using image processing techniques. The system utilized RGB color analysis with regression modeling, and experimental results showed that both the R and G channels exhibited strong predictive performance. The R channel achieved an R^2 of 0.985 with MAE of 0.398 mg/L and RMSE of 0.747 mg/L, while the G channel produced an R^2 of 0.969 with MAE of 0.535 mg/L and RMSE of 0.805 mg/L. The regression slopes 1.3779 for the R channel and 1.397 for the G channel indicate high system sensitivity to incremental changes in TAN concentration, while the estimated LOD, 0.155 mg/L and 0.215 mg/L for the R and G channels respectively, confirm that the prototype can detect TAN at low concentrations. Although the R channel exhibited slightly higher numerical accuracy, the G channel model provided superior operational stability, showing more consistent alignment with the identity line across the entire measurement range and reduced drift at higher TAN concentrations. This improved stability, together with its balanced sensitivity, acceptable LOD, and robust performance within the practical detection range of 0.2–2.0 mg/L, makes the G channel more suitable for integration into the embedded prototype system for monitoring applications. While the LOD of 0.215 mg/L exceeds chronic thresholds, the sensor effectively targets the acute toxicity window (>0.6 mg/L), serving as a vital screening tool for preventing fatal events. This positions the method as a robust solution for identifying immediate lethal threats rather than trace-level variations. Future optimizations will aim to extend sensitivity into the sub-lethal range (<0.1 mg/L) for comprehensive monitoring. The final prototype, incorporating a Raspberry Pi microcontroller, a controlled imaging chamber, and standardized illumination, provides a cost-effective, compact, and real-time solution for TAN monitoring. Furthermore, the integration with the LINE application offers aquaculturists immediate access to TAN data, enabling timely

decision-making and proactive water quality management. Compared to conventional spectrophotometric methods, the developed system presents a practical, affordable, and accessible alternative for small- and medium-scale aquaculture operations. By combining accuracy, operational robustness, and user accessibility, the proposed system enhances ammonia monitoring efficiency, mitigates toxicity risks, and supports the sustainable development of aquaculture industries.

[References]

[1] Sampantamit T, Ho L, Lachat C, Sutummawong N, Sorgeloos P, Goethals P. Aquaculture production and its environmental sustainability in Thailand: Challenges and potential solutions. Sustainability, 2020; 12(5): 2010. doi: 10.3390/su12052010.

[2] Eddy F B. Ammonia in estuaries and effects on fish. Journal of Fish Biology, 2005; 67(6): 1495–1513. doi: 10.1111/j.1095-8649.2005.00930.x.

[3] Camargo J A, Alonso Á. Ecological and toxicological effects of inorganic nitrogen pollution in aquatic ecosystems: A global assessment. Environment International, 2006; 32(6): 831–849.

[4] Isahak J, Thepahudi W, Jongcharoensuk R, Bia Kaeo T, Pan Dee T. Application of a webcam and image processing techniques for measuring total ammonia and nitrite concentrations in freshwater. RMUTSB Academic Journal, 2015; 3(2): 129–136. (in Thai)

[5] Molins-Legua C, Meseguer-Lloret S, Moliner-Martínez Y, Campíns-Falcó P. A guide for selecting the most appropriate method for ammonium determination in water analysis. TrAC Trends in Analytical Chemistry, 2006; 25(3): 282–290.

[6] Durborow R M, Crosby D M, Brunson M W. Ammonia in fish ponds. Southern Regional Aquaculture Center, SRAC publication, 1997; 463. Available: http://www.msstate.edu/dept/srac/fslist.htm. Accessed on [2025-]

[7] Zamora-Garcia I, Correa-Tome F E, Hernandez-Belmonte U H, Ayala-Ramirez V, Ramirez-Paredes J P. Mobile digital colorimetry for ammonia determination in aquaculture. Computers and Electronics in Agriculture, 2021; 181(1): 105960.

[8] Goldshleger N, Grinberg A, Harpaz S, Shulzinger A, Abramovich A. Real-time advanced spectroscopic monitoring of ammonia concentration in water. Aquacultural Engineering, 2018; 83(3): 103–108.

[9] Randall D J, Tsui T K N. Ammonia toxicity in fish. Marine Pollution Bulletin, 2002; 45(1-12): 17–23.

[10] Martins C I M, Eding E H, Verdegem M C J, Heinsbroek L T N, Schneider O, Blancheton J P, et al. New developments in recirculating aquaculture systems in Europe: A perspective on environmental sustainability. Aquacultural Engineering, 2010; 43(3): 83–93.

[11] Li H C, Yu K W, Lien C H, Lin C, Yu C R, Vaidyanathan S. Improving aquaculture water quality using dual-input fuzzy logic control for ammonia nitrogen management. Journal of Marine Science and Engineering, 2023; 11(6): 1109.

[12] Elmessery W M, Abdallah S E, Oraiath A A T, Espinosa V, Abuhussein M F A, Szűcs P, et al. A deep deterministic policy gradient approach for optimizing feeding rates and water quality management in recirculating aquaculture systems. Aquaculture International, 2025; 33(1): 253.

[13] Jiang F H, Tao J Y. UV-Visible spectrophotometric method for the determination of ammonia nitrogen using potassium bromate as oxidant. Desalination and Water Treatment, 2023; 306(1): 159–164.

[14] Ling T L, Ahmad M, Heng L Y. UV-vis spectrophotometric and artificial neural network for estimation of ammonia in aqueous environment using cobalt(II) ions. Analytical Methods, 2013; 5: 6709–6715. doi: 10.1039/C3AY40887F.

[15] Cho Y B, Jeong S H, Chun H, Kim Y S. Selective colorimetric detection of dissolved ammonia in water via modified Berthelot's reaction on porous paper. Sensors and Actuators B: Chemical, 2018; 256: 167–175. doi: 10.1016/j.snb.2017.10.069

[16] Tamim A T, Begum H, Shachcho S A, Khan M M, Yeboah-Akowuah B, Masud M, et al. Development of IoT based fish monitoring system for aquaculture. Intelligent Automation & Soft Computing, 2022; 32(1): 55–71.

[17] Amirjani A, Fatmehsari D H. Colorimetric detection of ammonia using smartphones based on localized surface plasmon resonance of silver nanoparticles. Talanta, 2018; 176: 242–246. doi: 10.1016/j.talanta.2017.08.022.

[18] Siribunbandal P, Kim Y H, Osotchan T, Zhu Z, Jaisutti R. Quantitative colorimetric detection of dissolved ammonia using polydiacetylene sensors enabled by machine learning classifiers. ACS Omega, 2022; 7(22): 18714–18721. doi: 10.1021/acsomega.2c01419.

[19] Soudi M, Cencillo-Abad P, Patel J, Ghimire S, Dillon J, Biswas A, et al. Self-assembled plasmonic structural color colorimetric sensor for smartphone-based point-of-care ammonia detection in water. ACS Applied Materials & Interfaces, 2024; 16(34): 45632–45639. doi: 10.1021/acsami.4c06615.

[20] Kamel A H, Abd‐Rabboh H S M. A dual-ion-selective electrode system for real-time monitoring of dissolved ammonia. Analyst, 2025; 18: 4145–4154. doi: 10.1039/d5an00647c.

[21] Chen Y, Goh S S, Damalerio R, Chen W, Choong D S W, Lim J Y C, et al. Development of long term stable multiple-ion- selective sensors for agriculture and aquaculture applications. Electronic Components and Technology Conference (ECTC), Orlando, FL, USA: IEEE, 2020; pp.997–1002. doi: 10.1109/ECTC32862.2020.00162

[22] Su X, Sutarlie L, Loh X J. Sensors, biosensors, and analytical technologies for aquaculture water quality. Research, 2020; 2020: 8272705.

[23] Endo H, Wu H. Biosensors for the assessment of fish health: A review. Fisheries Science, 2019; 85: 641–654.

[24] Siribunbandal P, Kim Y-H, Osotchan T, Zhu Z, Jaisutti R. Quantitative colorimetric detection of dissolved ammonia using polydiacetylene sensors enabled by machine learning classifiers. ACS Omega, 2022; 7(22): 18714–18721.

[25] Kilic V, Horzum N, Solmaz M E. From sophisticated analysis to colorimetric determination: Smartphone spectrometers and colorimetry. IntechOpen, 2018; doi: 10.5772/INTECHOPEN.82227.

[26] Kilic V, Alankus G, Horzum N, Mutlu A Y, Bayram A, Solmaz M E. Single-image-referenced colorimetric water quality detection using a smartphone. ACS Omega, 2018; 3(5): 5531–5536.

[27] Rani S, Biswas P C, Hossain A, Islam R, Canning J. Polynomial regression of multiple sensing variables for high-performance smartphone colorimeter. OSA Continuum, 2021; 4(2): 374–384.

[28] Mahmuda, Barkatullah, Haque E, Al Noman A, Ahmed F. Image processing based water quality monitoring system for biofloc fish farming. In: 2021 Emerging Technology in Computing, Communication and Electronics (ETCCE), Dhaka, Bangladesh: IEEE, 2021; pp.1–6, doi: 10.1109/ETCCE54784.2021.9689904.

[29] Phat N H, Hoan N D. Propose an automatic ammonia concentration of water measuring system combining image processing for aquaculture. Journal Européen des Systèmes Automatisés, 2021; 54(3): 453–460.

[30] Chicco D, Warrens M J, Jurman G. The coefficient of determination R-squared is more informative than SMAPE, MAE, MAPE, MSE and RMSE in regression analysis evaluation. PeerJ Computer Science, 2021; 7(3): e623.